gr-qc/0104066

Measurement of the gravitational constant G in space (Project SEE): sensitivity to orbital parameters and space charge effect

A.D. Alexeev[1], K.A. Bronnikov[2], N.I. Kolosnitsyn[3], M.Yu. Konstantinov[4], V.N. Melnikov[5]† and A.J. Sanders[6]‡

† *Russian Gravitational Society, 3-1 M. Ulyanovoy St., Moscow 117313, Russia*

‡ *Dept. of Physics and Astronomy, University of Tennessee, Knoxville, TN 37996-1200, USA*

We describe some new estimates concerning the recently proposed SEE (Satellite Energy Exchange) experiment for measuring the gravitational interaction parameters in space. The experiment entails precision tracking of the relative motion of two test bodies (a heavy "Shepherd", and a light "Particle") on board a drag-free space capsule. The new estimates include (i) the sensitivity of Particle trajectories and G measurement to the Shepherd quadrupole moment uncertainties; (ii) the measurement errors of G and the strength of a putative Yukawa-type force whose range parameter λ may be either of the order of a few meters or close to the Earth radius; (iii) a possible effect of the Van Allen radiation belts on the SEE experiment due to test body electric charging. The main conclusions are that (i) the SEE concept may allow one to measure G with an uncertainty smaller than 10^{-7} and a progress up to 2 orders of magnitude is possible in the assessment of the hypothetic Yukawa forces and (ii) van Allen charging of test bodies is a problem of importance but it may be solved by the existing methods.

1. Introduction

The SEE (Satellite Energy Exchange) concept of a space-based gravitational experiment was suggested in the early 90s [1] and was aimed at precisely measuring the gravitational interaction parameters: the gravitational constant G, possible violations of the equivalence principle measured by the Eötvös parameter η, time variations of G, and hypothetical non-Newtonian gravitational forces (parametrized by the Yukawa strength α and range λ). Such tests are intended to overcome the limitations of the current methods of ground-based experimentation and observation of astronomical phenomena and to fill gaps left by them. The significance of new measurements is quite evident since nearly all modified theories of gravity and unified theories predict some violations of the Equivalence Principle (EP), either by deviations from the Newtonian law (inverse-square-law, ISL) or by composition-dependent (CD) gravity accelerations, due to the appearance of new possible massive particles (partners); time variations of G (G-dot) are also generally predicted [2, 3].

Since gravitational forces are so very small, precision-measurement techniques have been at the core of terrestrial gravity research for two centuries. However, evidence is increasingly accumulating which indicates that terrestrial methods have plateaued in accuracy and are unlikely to achieve significant accuracy gains in the future. Ref. [4] describes the contemporary situation relative to the measurements of G and G-dot.

There is considerable evidence that the uncertainty in G has plateaued at about 100 ppm [5, 6, 7, 8]. Most of the stated errors in the recent experiments are of the order 100 ppm. Moreover, the scatter (1-sigma) about the mean is about 140 ppm. This conclusion does not include the recent paper by Gundlach and Merkowitz [9] who report an error of about 14 ppm in G measurement using a dynamically driven torsion balance. The reported value of G agrees with the previous measurements within their uncertainties. This work is unique for the moment and needs confirmation by other experimental groups using alternative methods.

It might seem that the problems of terrestrial apparatus must inexorably yield to new technologies — that the promise of ever increasing sensitivities would also lead to ever improving accuracy. However, this may not be true, since it is the intrinsically weak nature of the force and the resulting systematic errors which arise in its isolation and measurement that limit the ultimate attainable accuracy in terrestrial experiments [4].

The EP may be tested by searching for either violations of the inverse-square law (ISL) or composition-dependent (CD) effects in gravitational free fall.

In the watershed year of 1986, Fischbach et al. startled the physics community by showing that Eötvös's famous turn-of-the-century experiment is much less decisive as a null result than was generally believed [10, 11]. Prior to this time, experiments by Dicke [12] and

[1]e-mail: ada@mics.msu.su
[2]e-mail: kb@rgs.mccme.ru
[3]e-mail: nikkols@orc.ru
[4]e-mail: konstmyu@edward.netclub.ru
[5]e-mail: melnikov@rgs.phys.msu.su
Temporary address: CINVESTAV, Apartado Postal 14-740, Mexico 07360, D.F., Mexico; e-mail: melnikov@fis.cinvestav.mx
[6]e-mail: asanders@utkux.utcc.utk.edu

Braginsky [13] had demonstrated the universality of free fall (UFF) to very high accuracy with respect to several metals falling in the gravitational field of the Sun (the Eötvös parameter η was ultimately found to be smaller than 10^{-12}). The interpretation of these results at the time was that they validated UFF.

Since 1986 it has become customary to parametrize possible apparent EP violations as if due to a Yukawa particle with a Compton wavelength λ. This approach unites both ISL and CD effects very naturally, while the parameter values in the Yukawa potential suggest which experimental conditions are required to detect the new interaction.

Following the conjecture of Fischbach et al., ISL and CD tests were undertaken by many investigators. Although a number of anomalies were initially reported, nearly all of these were eventually explained in terms of overlooked systematic errors or extreme sensitivity to models, while most investigators obtained null results. However, a positive result for a deviation from the Newtonian law (ISL) was obtained (and interpreted in terms of a Yukawa-type potential) in the range of 20 to 500 m by Achilli and colleagues [14]; this needs to be verified in other independent experiments.

For reviews of terrestrial searches for non-Newtonian gravity, see [15, 16, 17].

The idea of the SEE method is to study the relative motion of two bodies on board a drag-free Earth satellite using horseshoe-type trajectories, previously well-known in planetary satellite astronomy: if the lighter body (the "Particle") is moving along a lower orbit than the heavier one (the "Shepherd") and approaching from behind, then the Particle almost overtakes the Shepherd, but it gains energy due to their gravitational interaction, passes therefore to a higher orbit and begins to lag behind. The interaction phase can be studied within a drag-free capsule (a cylinder up to 20 m long, about 1 m in diameter) where the Particle can loiter as long as 10^5 seconds. It was claimed that the SEE method exceeded in accuracy all other suggestions, at least with respect to G and α for λ of the order of meters. Some design features were considered, making it possible to reduce various sources of error to a negligible level. It was concluded, in particular, that the most favorable orbits are the sun-synchronous, continuous sunlight orbits situated at altitudes between 1390 and 3330 km [1].

Since the origination of the SEE concept, the development has focused on critical analyses of orbital parameters and satellite performance and the assessment of critical hardware requirements. All indications from this work are that the SEE concept is feasible and practicable [18].

At the present stage one can assert that, although space is a challenging environment for research, the inherent quietness of space can be exploited to make very accurate determinations of G and other gravitational parameters, providing that care is taken to understand the many physical phenomena in space which have the potential to vitiate accuracy. A distinctive feature of a SEE mission is its capability to perform such determinations simultaneously on multiple parameters, making it one of the most promising proposals.

To be more specific, let us enumerate the suggested SEE tests and measurements and show their expected accuracy as currently estimated:

Test/measurement	*Expected accuracy*
EP/ISL at a few metres	$2{\cdot}10^{-7}$
EP/CD at a few metres	$< 10^{-7}$ ($\alpha < 10^{-4}$)
EP/ISL at $\sim R_\oplus$	$< 10^{-10}$
G	$3.3{\cdot}10^{-7}$
$\dot{G}/G$	$< 10^{-13}$ in one year

The last estimate is only tentative; the subject is under study.

This paper presents a description of the main ideas of the SEE experiment and some new evaluations concerning the opportunities of the SEE concept and its yet-unresolved difficulties. In Sec. 2, on the basis of computer simulations of Particle trajectories, we describe some general properties of Particle trajectories in short (Particle-Shepherd separation from 2 to 5 meters) capsules, their sensitivity to the value of the parameters of the gravitational interaction, and we estimate the requirements to the Shepherd quadrupole moment uncertainty. Sec. 3 shows the results of simulations of the measurement procedure itself, which enables us to estimate the possible measurement accuracy with respect to G and α for λ of the order of either meters or the Earth's radius. Sec. 4 discusses a spurious effect of test body electric charging when the satellite orbit passes through the Van Allen radiation belts, rich in high-energy protons. Sec. 5 is a conclusion.

In what follows, the term "orbit" applies to satellite (or Shepherd) motion around the Earth, while the words "trajectory" or "path" apply to Particle motion with respect to the Shepherd inside the capsule.

2. Simulations of Particle trajectories

In the previous studies of the SEE project it was assumed that the capsule was about 20 m long and the initial Shepherd-Particle separation x_0 along the capsule axis was as great as 18 m; some estimations were also made for 5 m $\le x_0 \le$ 10 m. The Shepherd mass was taken to be $M = 500$ kg and the Particle mass $m = 0.1$ kg. The present study retains these values, except the cases noted below.

In this section we will describe some characteristic features of Particle trajectories in a short capsules (Particle-Shepherd separation 2 m $\le x_0 \le$ 5 m) with the Shepherd mass reduced to $M = 200$ kg. Our goal is to determine the properties of trajectories in the case considered and to determine the sensitivity of trajectories to the uncertainty of orbit radius, the value of the Newtonian gravitational constant and of the Shepherd quadrupole moment J_2. As in our previous studies, the capsule diameter is presumed to be 1 m.

The reason for considering the short capsule, the Shepherd with reduced mass and the quadrupole moment uncertainty is economical and technological in origin. Namely, it is hard to produce a spherically symmetric Shepherd to the required accuracy. To avoid the inclusion of δJ_2 in the set of parameters to be determined in the experiment, it is useful to know which values of δJ_2 will be negligible, since the growth of the number of parameters leads to serious problems in data processing.

2.1. Equations of motion and initial data

For simplicity, we assume that the relative motion of the test bodies inside the capsule occurs in the satellite orbital plane. This simplification is purely technical, since, as was found in our previous studies, the three-dimensional nature of the Particle motion does not change the main estimates.

The reduced Lagrangian of the Particle motion in the considered case is

$$L = \frac{M}{2}(\dot R^2 + R^2\dot\varphi^2) + \frac{m}{2}\left[\dot r^2 + r^2(\dot\varphi+\dot\psi)^2\right] + G\frac{M_\oplus m}{r} + G\frac{Mm}{s}\left\{1 + J_2\left(\frac{r_s}{s}\right)^2 P_2(\cos\theta)\right\}\left(1+\alpha e^{-s/\lambda}\right) \quad (1)$$

where (R,φ) are the Earth-centered polar coordinates of the Shepherd in the orbital plane; $r = \sqrt{(R+y)^2+x^2}$ and ψ are the Earth-centered polar coordinates of the Particle; x and y are the Shepherd-centered Particle coordinates, where x is the "horizontal" one, i.e., along the orbit and simultaneously along the capsule and y is the "vertical" one, along the Earth-Shepherd radius vector; $s = \sqrt{x^2+y^2}$ is the Particle-Shepherd separation; $M_\oplus$, M and m are the Earth, Shepherd and Particle masses, respectively; J_2 is the quadrupole moment of the Shepherd, r_s is its radius and P_2 is the Legendre polynomial

$$P_2(\cos\theta) = \frac{3\cos^2\theta - 1}{2},$$

where θ is the angle between the line connecting the centres of test bodies and the Shepherd equatorial plane. It is easy to see that if the Shepherd symmetry axis is in its orbital plane, then $\theta = \theta_0 = -\arctan(y/x) + \varphi$. If the symmetry axis of the Shepherd is orthogonal to its orbital plane, then $\theta = 0$. In general, if χ is the angle between the Shepherd symmetry axis and its orbital plane, then $\theta = \theta_0\cos\chi$. Hence the influence of J_2 on the Particle motion is minimum if the Shepherd symmetry axis lies in its orbital plane and is maximum if they are mutually orthogonal.

For simplicity (and taking into account the corresponding estimate) we neglect the influence of the Particle on the Shepherd, so the Shepherd trajectory is considered as given. Then, varying the above Lagrangian with respect to x and y, taking into account that $M \gg m$ and $R \gg s$, we arrive at the following equations of Particle motion with respect to the Shepherd:

$$\begin{aligned}\frac{d^2x}{dt^2} &= 2\dot y\dot\varphi + x\left\{\dot\varphi^2 - \frac{GM_\oplus}{r^3}\right\} - \frac{2\dot R\dot\varphi y}{R} - \frac{G\overline{M}}{s^3}x\left\{1 + J_2\left(\frac{r_s}{s}\right)^2 P_2(\cos\theta)\right\} \\ &\quad - \alpha x\frac{G\overline{M}}{s^2}\left\{1 + J_2\left(\frac{r_s}{s}\right)^2 P_2(\cos\theta)\right\}\left(\frac{1}{s}+\frac{1}{\lambda}\right)\mathrm{e}^{-s/\lambda} \\ &\quad + \frac{G\overline{M}r_0^2}{2s^5}J_2\left(1+\alpha\,\mathrm{e}^{-s/\lambda}\right)\times\left[x(1+3\cos 2\theta) + 3y\sin 2\theta\cos\chi\right]; \quad (2)\end{aligned}$$

$$\begin{aligned}\frac{d^2y}{dt^2} &= -2\dot x\dot\varphi + (R+y)\left\{\dot\varphi^2 - \frac{GM_\oplus}{r^3}\right\} + \frac{2\dot R\dot\varphi x}{R} - \frac{G\overline{M}}{s^3}y\left\{1 + J_2\left(\frac{r_s}{s}\right)^2 P_2(\cos\theta)\right\} \\ &\quad - \alpha y\frac{G\overline{M}}{s^2}\left(\frac{1}{s}+\frac{1}{\lambda}\right)\left\{1 + J_2\left(\frac{r_s}{s}\right)^2 P_2(\cos\theta)\right\}\mathrm{e}^{-s/\lambda} \\ &\quad + \frac{G\overline{M}r_0^2}{s^5}J_2\left(1+\alpha\,\mathrm{e}^{-s/\lambda}\right)\times\left[3x\sin 2\theta\cos\chi + y(1-3\cos\theta)\right] \quad (3)\end{aligned}$$

where $\overline{M} = M + m$.

Two kinds of initial conditions for Eqs. (2) and (3) were used during the simulations. First, we used the so-called "standard" initial conditions, taking the Particle velocity components $\dot{x}(0)$ and $\dot{y}(0)$ corresponding to its unperturbed (i.e., without the $M-m$ interaction) orbital motion distinguished from the Shepherd's orbit only by its radius (for circular orbits) or semimajor axis (for elliptic orbits). Assuming that the Particle motion begins right at the moment when the Shepherd passes its perigee, these conditions have the form

$$\begin{aligned} x(0) &= x_0, \qquad y(0) = y_0, \\ \dot{x}(0) &= \frac{\omega e' y_0}{2(1-e)^2}, \qquad \dot{y}(0) = -\frac{\omega e x_0}{e'(1-e)} \end{aligned} \tag{4}$$

where $\omega^2 = GM_\oplus/R_0^3$, R_0 is the Shepherd orbital radius (at the perigee), e is the orbital eccentricity and $e' = \sqrt{1-e^2}$.

For clearness, the relations (4) are written in the linear approximation in the variables x and y. Higher-order approximations were used in the simulation process as well.

The second kind of initial conditions corresponds to small variations of initial velocities with respect to their "standard" values.

The set of equations (2)–(3) was solved numerically using the software developed previously [18] to analyze the SEE project.

On the basis of numerical solutions of Eqs. (2) and (3), we considered two types of Particle trajectories, corresponding to different choices of the initial data: (i) approximately U-shaped ones and (ii) cycloidal ones, containing loops (see more details on the trajectories in [1, 18]), for orbital altitudes $H_{\rm orb} = 500$, 1500 and 3000 km.

2.2. General characteristics of trajectories in a short capsule

Reduction of the Shepherd mass leads to the reduction of distance between libration points L_1 and L_2. As a result, the region where the horseshoe orbits exist is reduced as well, and the turning points for the horseshoe orbits become closer to the Shepherd. Thus, for a Shepherd mass of $M = 200$ kg, the positions of the turning points of the horseshoe orbits starting, for instance, at $x_0 = 18$ m and 0.1 m$\leq |y_0| \leq 0.3$ m are placed in the region $x \leq 5$ m for all orbits whose altitude H is in interval 500 km $\leq H \leq 3000$ km. The usage of short trajectories, which start in the region $x_0 \leq 5$ m, and especially extremely short trajectories with $x_0 = 2$ m, leads to additional limitations on the initial conditions.

Numerical simulation shows that to avoid Particle collisions with the Shepherd and the walls of the capsule for "smooth" trajectories, which correspond to the standard initial conditions, trajectories with $|y_0| \leq 0.2$ m may be used for orbit altitudes $H_{\rm orb} \leq 1500$ km while for orbit altitude $H_{\rm orb} = 3000$ km and $x_0 \geq 3$ m trajectories with $|y_0| = 25$ cm may be used also.

The usage of cycloidal trajectories, which appear when the absolute values of the Particle's initial velocity exceed its standard value, make it possible to avoid this limitation.

2.3. Trajectory sensitivity with respect to the Newtonian gravitational constant

The influence of the Newtonian gravitational constant G on the Particle motion in the case considered may be investigated by considering how a small perturbation δG from the "standard" value of G changes the Particle trajectories. Such a perturbation is characterized by the displacement of a perturbed trajectory with respect to an unperturbed one, that is,

$$\delta\vec{r} = \vec{r}_\delta(t) - \vec{r}_0(t)$$

where $\vec{r}_\delta$ and $\vec{r}_0$ denote the Particle radius vector for perturbed and unperturbed motion, respectively. For rather long trajectories, instead of the full displacement $\delta\vec{r}$, the displacement along the x axis (δx) may be considered, because a numerical simulation shows that a displacement along the y axis is one order of magnitude smaller than a displacement along the x-axis.

U-shaped Particle trajectories were considered for circular Shepherd orbits in the following range of parameters and initial conditions: orbit altitudes $H_{\rm orb} =$ 500, 1500 and 3000 km; the initial position changes in the range 2 m $\leq x_0 \leq$ 5 m, -20 cm $\leq y_0 \leq -5$ cm. For comparison with the case where $M = 500$ kg, trajectories with $x_0 = 18$ m were considered also. It was found that the perturbation $\delta G/G = 10^{-6}$ leads to displacement of smooth trajectories in the range from $0.634{\cdot}10^{-6}$ m to $3.34{\cdot}10^{-6}$ m with a minimum displacement achieved for $y_0 = 0.05$ m, $x_0 = 2$ m and $H_{\rm orb} =$ 3000 km while a maximal displacement is achieved for $y_0 = 0.05$ m, $x_0 = 5$ m and $H_{\rm orb} = 500$ km.

The use of cycloidal trajectories increases the influence of δG on the Particle motion.

2.4. Trajectory sensitivity to the orbit radius uncertainty

This sensitivity is characterized by the displacement δx, induced by a small perturbation (or uncertainty) δh of the orbital altitude [1] $H_{\rm orb}$.

It was found that for $\delta h = 1$ cm, the orbital altitude $H_{\rm orb} = 1500$ km and $|y_0| = 20$ cm, the maximum value of δx increases from $3.222 \cdot 10^{-8}$ m at $x_0 = 2$ m to $9.387 \cdot 10^{-8}$ m at $x_0 = 5$ m. For $H_{\rm orb} = 500$ km these values must be multiplied by a factor of 2

[1] As above, we consider the displacement δx instead of δr because δx provides the main contribution to δr, while δy is much smaller.

Table 1. Estimates of $\delta G/G$ in ppm for $\delta J_2 = 10^{-4}$, when the symmetry axis of the Shepherd is orthogonal ($\chi = \pi/2$) to its orbital plane. The second line shows x_0.

y_0,	x_0			
cm	2 m	3 m	4 m	5 m
-5	1.568	5.13	2.41	0.138
-10	3.181	1.41	0.876	0.649
-15	0.857	6.08	5.057	4.486
-20	60.28	44.31	31.91	28.04

(approximately) and for $H_{\rm orb} = 3000$ km by a factor of 1/2.

It was also found that the dependence $\delta x(\delta h)$ is, to a good accuracy, linear: in particular, for $\delta h = 1$ m, the orbital altitude $H_{\rm orb} = 1500$ km, $x_0 = 5$ m and $|y_0| = 20$ cm, $\delta x = 9.387 \cdot 10^{-6}$ m as expected.

The use of cycloidal trajectories reduces the dependence of trajectories on the orbit altitude: for instance, for $H_{\rm orb} = 1500$ km, $x_0 = 5$ m and $|y_0| = 20$ cm, the uncertainty $\delta h = 1$ cm leads to $\delta x = 1.455 \cdot 10^{-8}$ m.

It is necessary to point out that the influence of the orbital altitude on the Particle trajectory for the reduced Shepherd mass ($M = 200$ kg) is greater than in the case $M = 500$ kg. For instance, in the case $M = 500$ kg, $H_{\rm orb} = 1500$ km, $\delta h = 1$ m, $x_0 = 5$ m and $|y_0| = 20$ cm, the trajectory displacement becomes $\delta x = 4.6593 \cdot 10^{-8}$ m.

These estimates lead to certain restrictions on the reasonable precision of Particle trajectory measurements.

2.5. Trajectory sensitivity to the Shepherd's quadrupole moment uncertainty

A maximum effect of the Shepherd quadrupole moment J_2 on the Particle motion is realized in the case when the Shepherd axis is orthogonal to its orbital plane. The influence of δJ_2 on the accuracy of G measurement may be estimated as follows. Let some value of δJ_2 produce the trajectory displacement $|\delta\vec{r}| \le \delta l_j$ while the variation δG_0 of G with the same initial conditions gives the trajectory displacement $|\delta\vec{r}| \le \delta l_G$. Then, keeping in mind the linear dependence of trajectory displacements on δJ_2 and δG, the accuracy of G measurement under the uncertainty δJ_2 may be estimated as

$$\frac{\delta G}{G} \le \left(1 + \frac{\delta l_j}{\delta l_G}\right)\frac{\delta G_0}{G}.$$

Using this inequality and the results of trajectory simulations, we obtain the following estimates for U-shaped Particle trajectories in circular orbits with $H_{\rm orb} = 1500$ km:

The uncertainties $\delta J_2 \lesssim 10^{-5}$ do not create a substantial error in G for most of the trajectories. Only trajectories with $|y_0| = 0.2$ m require $\delta J_2 \lesssim 10^{-6}$ because of the growth of the sinusoidal component for these trajectories.

3. Simulations of experimental procedures

This section describes the results of numerical simulations of the whole measurement procedures aimed at obtaining the sought-after gravitational interaction parameters. These simulations assumed a Shepherd mass of $M = 500$ kg, a circular orbit with $H_{\rm orb} = 1500$ km with a spherical gravitational potential for the Earth, and a Particle mass of 100 g. Where relevant, it is assumed that both the Shepherd and the Particle are made of tungsten. Identical compositions for them are assumed for simplicity since this work is performed for estimation purposes only.

3.1. Simulations of an experiment for measuring G

The constant G is determined from the best fitting condition between the "theoretical" Particle trajectories ($\vec{r}^{\,\rm th}(t_i) = \vec{r}_i^{\,\rm th}$), calculated by Eqs. (2) and (3) for $J_2 = 0$ and the "empirical" ($\vec{r}_i$) Particle trajectories near the Shepherd. The fitting quality is evaluated by minimizing a functional that characterizes a "distance" between the trajectories. We have considered the following functionals for such "distances":

$$S = \sum_{i=1}^{N}\left[(x_i - x_i^{\rm th})^2 + (y_i - y_i^{\rm th})^2\right], \qquad (5)$$

$$S_x = \sum_{i=1}^{N}(x_i - x_i^{\rm th})^2, \qquad S_y = \sum_{i=1}^{N}(y_i - y_i^{\rm th})^2, \qquad (6)$$

The theoretical trajectory depends on the gravitational constant G, on the initial coordinates x_0, y_0 and on the initial velocities v_{x0}, v_{y0}. To estimate G, one chooses the value for which a "distance" functional in the space of the five variables $(G, x_0, y_0, v_{x0}, v_{y0})$ reaches its minimum.

We carried out a numerical simulation of the SEE experiment and estimated δG for a given coordinate measurement error ($\sigma = 1 \cdot 10^{-6}$ m). As "empirical" trajectories, we took computed trajectories, with specified values of the above five variables, where Gaussian noise was introduced from a random number generator. Independent "empirical" trajectories were created by non-intersecting random number sequences. The functional was minimized using the gradient descent method and the consecutive descent method. The starting value of the "vertical" (along the Earth's radius)

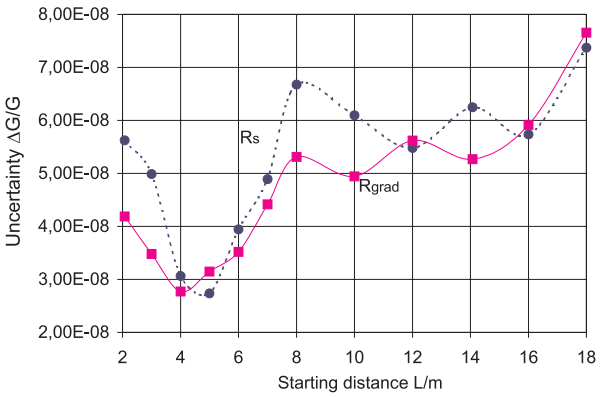

Figure 1: Uncertainties δG estimated by the gradient descent ($R_{\rm grad}$) and consecutive descent ($R_{\rm s}$) methods.

coordinate, y_0, was taken to be 0.25 m, while the horizontal one, x_0, varied between 2 and 18 m. Fig 1 shows the dependence of the errors $\delta G/G = R_{\rm grad}$, obtained by the gradient descent method and $\delta G/G = R_{\rm s}$, obtained by the consecutive descent method. All the errors are estimated by confidence intervals corresponding to a confidence of 0.95. The mean values of these errors are as follows:

$$R_{\rm grad} = 4.69{\cdot}10^{-8}, \qquad R_{\rm s} \;=\; 5.24{\cdot}10^{-8}.$$

Thus the errors estimated by the gradient and consecutive descent methods are close to each other and are about an order of magnitude smaller than the error from one-trajectory data. It was found that the simulation results depend strongly on the random number generator, so that ordinary generators are not perfect: the generated random number sets do not obey the Gaussian law.

The use of truncated functionals like (2) has shown that a functional incorporating the more informative "horizontal" coordinate x leads to estimates close to those obtained from the total functional, whereas the use of y alone substantially decreases the sensitivity. Therefore in practice, to determine G, it is sufficient to measure only one of the two coordinates, viz. x.

Since the "empirical" trajectory is built on the basis of a computed one, with a known value of the gravitational constant G_0, it appears possible to estimate a possible systematic error inherent in the data processing method. The latter has turned out to be in most cases much smaller than the random error. This result shows the correctness of the methods used.

As is evident from the results, the best accuracy is achieved at values of x_0 ($\approx$ the capsule size) about 4–5 meters.

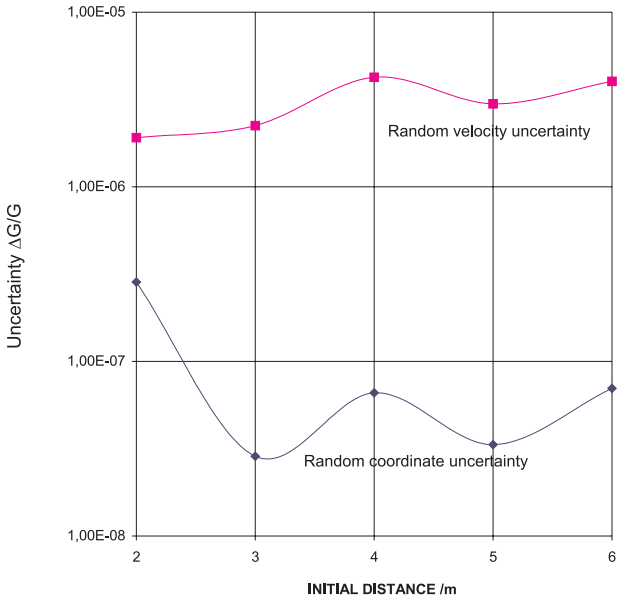

Figure 2: Random "velocity" and "coordinate" uncertainties.

3.2. Simulation of measurement procedures for estimation of G using velocity data

When one can precisely measure the Particle velocity, the gravitational constant can be estimated from the velocity data alone. A computer program was created for simulating an experiment determining the gravitational constant G by velocity data. These simulations assumed a Shepherd mass of 500 kg, a circular orbit with $H_{\rm orb} = 1500$ km (spherical Earth's potential), a Particle mass of 100 g, and a velocity error $\delta v_x = 1 \cdot 10^{-8}$ m/s. The constant G is estimated from the best fitting condition between the theoretical Particle velocity $\left(\vec{v}^{\,\rm th}(t_i) \equiv \vec{v}_i^{\,\rm th}\right)$ and the empirical one. The fitting quality is evaluated by minimizing a functional characterizing a distance between velocity trajectories. We used the following functional:

$$V = \sum_{i=1}^{N} \left[\left(v_{xi} - v_{xi}^{\rm th}\right)^2 + \left(v_{yi} - v_{yi}^{\rm th}\right)^2 \right].$$

The theoretical velocity depends on the gravitational constant G, on the initial coordinates x_0, y_0 and the initial velocities v_{x0}, v_{y0}. To estimate G, one chooses the value for which the velocity distance functional V reaches its minimum in the space of the five variable $(G, x_0, y_0, v_{x0}, v_{y0})$

As empirical trajectories, we took computed trajectories with specified values of the above five variables, where Gaussian noise was introduced from a random number generator. Independent empirical trajectories were created by non-intersecting random number sequences. The functional V was minimized using the gradient descent method. The starting value of the y_0

coordinate was taken to be 0.25 m, while the horizontal one, x_0, varied between 2 and 6 m. The value of G was estimated from 11 trajectories at a significance level of 0.95. The appropriate errors were estimated at confidence intervals and then related to G as shown by the upper curve in Fig. 2. The relative error obtained using the coordinate functional for a coordinate measurement error of $\sigma = 1\cdot10^{-6}$ m is also shown in the same figure. Computer-based simulation also allows one to estimate systematic errors. We see that the accuracy of estimation of G for a given set of measurement errors is the best for the coordinate functional.

3.3. Equations of motion with Yukawa terms

We will present the Particle equations of motion in the relevant approximation, including the contributions from hypothetical Yukawa forces, taking into account the finite size of the Yukawa field sources.

Let the interaction potential for two elementary masses m_1 and m_2 be described by the potential

$$dV^{\rm Yu} = \frac{G\,dm_1 dm_2}{r}\alpha\,{\rm e}^{-r/\lambda} \tag{7}$$

where r is the masses' separation, α and λ are the strength parameter and the range of the Yukawa forces. Then for two massive bodies with the radii R_1 and R_2 after integration over their volumes we obtain [20]

$$V^{\rm Yu} = \frac{G\,m_1 m_2 \beta_1\beta_2}{r}\alpha\,{\rm e}^{-r/\lambda} \tag{8}$$

where

$$\beta_i = 3\left(\frac{\lambda}{R_i}\right)^3\left[\frac{R_i}{\lambda}\cosh\frac{R_i}{\lambda} - \sinh\frac{R_i}{\lambda}\right]. \tag{9}$$

When $R_i/\lambda \ll 1$, we have $\beta_i \approx 1$. This may be the case when we consider the interaction between the Shepherd and the Particle at a distance of the order of a few meters. The radii of the Shepherd and the Particle are small: $R_1 \approx 18$ cm for the Shepherd and $R_2 \approx 1.1$ cm for the Particle. If the range λ is of the order of the Earth radius, $\lambda \approx R_\oplus$, we have $\beta_\oplus = 1.10$ and $\beta_{1,2} = 1$ where the indices 1 and 2 label the Shepherd and the Particle, respectively.

Equations of motion are obtained under the following assumptions. There are two Yukawa interactions with the parameters λ_0 and α_0 referring to the Earth-Shepherd and Earth-Particle interactions which are the same (due to the assumed identical composition for the Shepherd and the Particle), while λ and α determine the Shepherd-Particle interaction. The equations of motion in the frame of reference of the Shepherd, with the same notations for x, y and s as used previously, are

$$\ddot{x} + 2\omega^2\dot{y} + G(m_1+m_2)\frac{x}{s^3} - 3\omega^2\frac{xy}{s} + G(m_1+m_2)\frac{x}{s^3}\alpha\left(1+\frac{s}{\lambda}\right){\rm e}^{-s/\lambda} = 0;$$

$$\ddot{y} - 2\omega\dot{x} - 3\omega^2 y + G(m_1+m_2)\frac{y}{s^3} + \frac{3\omega^2}{r_{01}}\left(y^2 - \frac{x^2}{2}\right) + G(m_1+m_2)\frac{y}{s^3}\alpha\left(1+\frac{s}{\lambda}\right){\rm e}^{-s/\lambda} - \omega^2\beta_0\alpha_0\,{\rm e}^{-r_{01}/\lambda_0}y = 0 \tag{10}$$

where ω is the orbital frequency:

$$\omega^2 = \frac{GM_\oplus}{r_{01}^3}\left[1 + \beta_0\alpha_0\left(1+\frac{r_{01}}{\lambda_0}\right){\rm e}^{-r_{01}/\lambda_0}\right]. \tag{11}$$

We have neglected the terms quadratic in s/r_{01} times α or α_0 due to their manifestly small contributions.

If we set $\alpha_0 = 0$ in Eqs. (10), we obtain the equations used to describe only the Shepherd-Particle Yukawa interaction. Notice that the Yukawa terms are roughly proportional to the gradients of the corresponding Newtonian accelerations, namely, Gm_1/s^3 for the Shepherd-Particle interaction and $GM_\oplus/r_{01}^3 \approx \omega^2$ for (say) the Earth-Shepherd interaction. In our case these quantities are estimated as

$$\frac{Gm_1}{s^3} \approx 2.7\cdot10^{-10}\ {\rm s}^{-2} \qquad \text{for} \quad s = 5\ {\rm m},$$
$$\text{and} \quad \omega^2 \approx 8.16\cdot10^{-7}\ {\rm s}^{-2}. \tag{12}$$

Thus, given the same strength parameter, the Earth's Yukawa force is three orders of magnitude greater than that between the Shepherd and the Particle. Therefore, one might expect some significant progress in an ISL test for λ of the order of the Earth's radius.

Eqs. (10) were used to simulate the measurement procedures.

3.4. Sensitivity to Yukawa forces with $\lambda \sim 1$ m

In an experiment for finding the Yukawa interaction between the Shepherd and the Particle using the potential (8) with $\beta_{1,2} = 1$, one computes two theoretical trajectories: the first ignoring the Yukawa forces $(x^0(t_i),\ y^0(t_i))$ and the second taking them into account $\left(x^\alpha(t_i),\ y^\alpha(t_i)\right)$. These two computed curves are compared with the empirical trajectory using the functional S_k $(k = 0, \alpha)$ according to (5) which may be considered as a dispersion characterizing a scatter of the "empirical" coordinates with respect to the fitting trajectory. This is true when the theoretical model is adequate to the real situation. In the case $k = \alpha$ the functional $S_k = s_\alpha$ has a χ^2 distribution with $n_2 = 2N-1$ degrees of freedom. With $k = 0$ the parameter α is absent, therefore S_0 is distributed according to the χ^2 law with $N_1 = 2N$ degrees of freedom. Then their ratio $S_0/S_\alpha = F_{n_2,n_1}$ will be distributed according to the Fischer law [27] with n_2 and n_1 degrees of freedom. If

an experiment shows that, on a given significance level q, the relation (see [11])

$$S_0/S_\alpha \geq F_{n_1,n_2,q} \tag{13}$$

is valid, one should conclude that the Yukawa force has been detected. An equality sign shows a minimum detectable force for the given significance level q. We have assumed $q = 0.95$. The results of a sensitivity computation for different values of the space parameter λ are presented in Fig. 3 (curve 1). A maximum sensitivity of $\alpha = 2.1{\cdot}10^{-7}$ has been observed for $\lambda = 1.25$ m. This value is 3 to 4 orders of magnitude better than the sensitivity of terrestrial experiments in the same range.

3.5. Sensitivity to Yukawa forces with $\lambda \sim R_\oplus$

To estimate the parameter α_0 in Eqs. (10), computer simulations were carried out using the method as described above for α, based on the Fischer criterion for the significance level 0.95. The range parameter λ_0 varied from $(1/32)R_\oplus$ to $32R_\oplus$. Two trajectories with the initial Shepherd-Particle separations x_0 of 2 and 5 m were calculated. In both cases the impact parameter y_0 was chosen to be 0.25 m. We used Eqs. (10) with $\alpha = 0$, i.e., excluding the non-Newtonian interaction between the Shepherd and the Particle. As is evident from Eqs. (10), the Particle trajectory depends on the ratio r_{01}/λ_0 in the product $(r_{01}/\lambda_0)\,\mathrm{e}^{-r_{01}/\lambda_0}$. This quantity reaches its maximum at $\lambda_0 = r_{01}/2$. Our calculations have confirmed that a maximum sensitivity of the SEE method ($3.4{\cdot}10^{-8}$ for $x_0 = 5$ m) is indeed observed at this value of λ_0 . This is about an order of magnitude better than the estimates obtained by other methods. Hopefully this estimate may be further improved by about an order of magnitude by optimization of the orbital parameters. However, there is a factor which can, to a certain extent, spoil these results, namely, the uncertainty in the parameter ω which, in this calculation, was assumed to be known precisely.

The simulation results are shown in Fig. 3 (curve 2) for a trajectory with an initial Shepherd-Particle separation of 5 metres. See the next section for further discussion of this figure.

3.6. Precession of the Shepherd orbit and a test of the Inverse Square Law at distances of the order of $R_\oplus$

We have shown previously that the SEE experiment allows one to test the inverse square law at distances on the order of 1 m ($\alpha_{\min} \sim 2 \cdot 10^{-7}$) and at distances on the order of a half of an orbit radius ($\alpha_{\min} \sim 3.4{\cdot}10^{-8}$) [25]. Another test can be done using spacecraft precession data. As known, in two-body problems an orbit is closed for only two potentials. They are (1) the Newtonian potential, $U \sim 1/r$, and (2) $U \sim r^2$. In other cases the orbit is not closed and a pericenter precession is observed. In particular, any deviation from the Newtonian law entails a precession of an orbit due to the Yukawa interaction

$$U' = \frac{Gm_1m_2}{r}\alpha\,\mathrm{e}^{-r/\lambda} \tag{14}$$

the Shepherd orbit exhibits a precession. In the general case the precession magnitude due to a small perturbation, described by a potential δU, is given by (see [1])

$$\delta\varphi = \frac{\partial}{\partial M}\left(\frac{2m'}{M}\int_0^\pi r^2\delta U\,d\varphi\right) \tag{15}$$

Integration is done over a non-perturbed trajectory. Here m is the Shepherd's mass, m' is the mass of a central body (the Earth), $M = mr^2\dot\varphi$ is an integral of motion (the angular momentum), and $\delta U = \alpha(Gmm')\,\mathrm{e}^{-r/\lambda}$. The non-perturbed trajectory is described by the expressions

$$\begin{aligned} r &= \frac{p}{1+e\cos\varphi}, \qquad p = \frac{M^2}{m(Gmm')} \\ e^2 &= 1 + \frac{2EM^2}{m(Gmm')^2}p = a(1-e^2). \end{aligned} \tag{16}$$

After a standard algebraic computation we obtain

$$\begin{aligned} \delta\varphi = \alpha\frac{2}{e}\int_0^\pi &\frac{\mathrm{e}^{-r/\lambda}}{(1+e\cos\varphi)^2} \\ &\times\left\{\frac{1}{\lambda}\left[2e+(1+e^2)\cos\varphi\right]-(e+\cos\varphi)\right\}d\varphi, \end{aligned} \tag{17}$$

where

$$\frac{r}{\lambda} = \frac{a}{\lambda}\cdot\frac{1-e^2}{1+e\cos\varphi}. \tag{18}$$

Using Eq. (8) and data with the error $\delta\varphi$ for the SEE Satellite, we calculated the curves $\alpha(\lambda)$, which determine the border on the $\alpha-\lambda$ plane between two domains, where the Yukawa interaction (a new long-range force) is forbidden by experiment and where it is not. The sensitivities to Yukawa interactions are shown in Fig. 3 as the curve 4 (see [10]) for the parameter λ in the range from $1 \cdot 10^6$ m to $1 \cdot 10^{13}$ m. The curve 3 was calculated for the SEE satellite with an eccentricity $e = 0.01$ and the precession error is equal to $\delta\varphi = 0.1''/y$.

One can conclude that the inverse square law may be tested with a sensitivity of $\alpha \sim 6.3{\cdot}10^{-11}$ for $\lambda \sim 3.9{\cdot}10^6$ m (half the orbital radius).

4. A possible effect of the Earth's radiation belt

Charged particles, penetrating into the SEE capsule from space and captured by the test bodies, create electrostatic forces that could substantially distort the experimental results. Among the sources of such particles

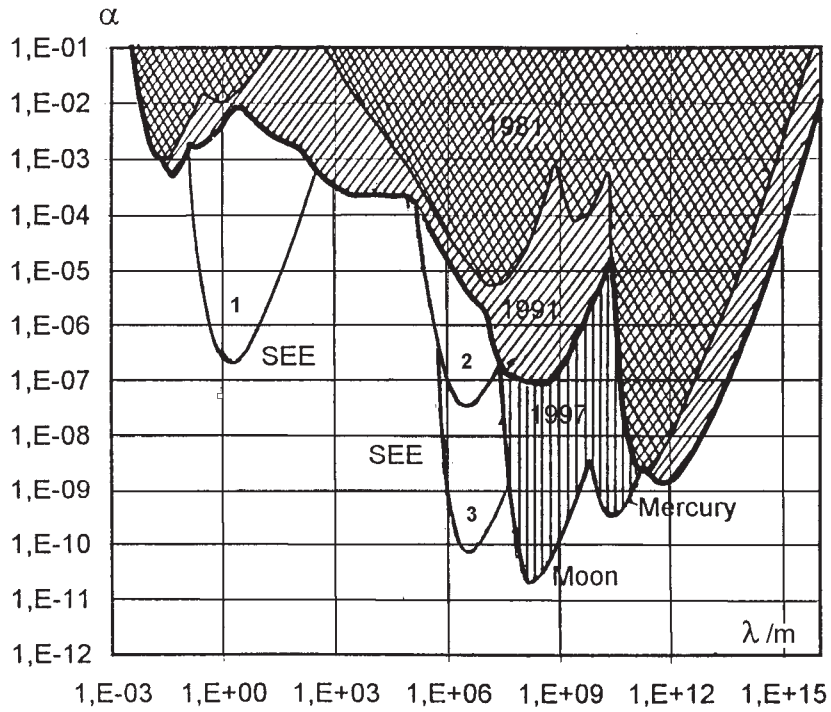

Figure 3: The SEE method sensitivity to Yukawa forces with the range parameter λ_0 of the order meters (1) of the Earth's radius $R_\oplus$ using trajectory measurements (2) and orbit precession (3). The limitations on Yukawa's forces parameters from [11] (4).

one should mention (i) cosmic-ray showers, (ii) solar flares and (iii) the Earth's radiation belts (Van Allen belts). The effect of cosmic-ray showers was estimated in Ref. [1] and shown to be negligible. Solar flares are more or less rare events and, although they create very significant charged particle fluxes, sometimes even exceeding those in the most dense regions of the radiation belts, one can assume that the SEE measurements (except those of $\dot{G}$) are stopped for the period of an intense flare. On the contrary, the effect of the Van Allen belts is permanent as long as the satellite orbit passes, at least partially, inside them.

We will show here that the charging is unacceptably high at otherwise favorable satellite orbits, so that some kind of charge removal technique is necessary, but this problem may be addressed rather easily by presently available technology.

The range of the most favorable SEE orbital altitudes, roughly 1400 to 3300 km [1], coincides with the inner region of the so-called inner radiation belt [21–24], situated presumably near the plane of the magnetic equator. This region is characterized by a considerable flux of high-energy protons and electrons. For a SEE satellite at altitudes near 1500 km the duration of the charging periods is about 12 minutes. Maximum charging rates occur in the central Atlantic. It should be noted that the South Atlantic Anomaly (SAA) — a region of intense Van Allen activity which results from the low altitude of the Earth's magnetic field lines over the South Atlantic Ocean — cannot cause additional problems for the SEE experiments. The reason is that the SAA mostly contains low-energy protons which cannot penetrate into the SEE capsule.

Electrons are known to be stopped by even a thin metallic shell, so only protons are able to induce charges on the test bodies. Proton-induced charges on the test bodies can create considerable forces. The inner radiation belt contains protons with energies of 20 to 800 MeV, and their maximum fluxes at an altitude of 3000 km over the equator are as great as about $3{\cdot}10^6\,\mathrm{cm^{-2}s^{-1}}$ for energies $E \gtrsim 10^6$ eV and about $2{\cdot}10^4\,\mathrm{cm^{-2}s^{-1}}$ for $E \gtrsim 10^7$ eV. At 1500 km altitude these numbers are a few times smaller; the fluxes gradually decrease with growing latitude φ and actually vanish at $\varphi \sim 40^\circ$.

It is important that estimates of any resulting effects take into account that (i) the capsule walls have a considerable thickness and stop the low-energy part of the proton flux and (ii) among the protons that penetrate the capsule and hit the Particle, the most energetic ones, whose path in the Particle material is longer than the Particle diameter, fly it through and hit the capsule wall again. As for the Shepherd, its size is large enough to stop the overwhelming majority of protons which hit it.

In what follows, we will assume a Shepherd radius

of 20 cm and a Particle radius of 2 cm and estimate the captured charges for some satellite orbits in a capsule whose walls of aluminium are 2, 4, 6 and 8 cm thick. The SEE satellite must actually involve several coaxial cylinders for thermal-radiation control, and the combined thickness of their walls must amount to several cm. We will assume, in addition, that the Particle also consists of aluminium and stops all protons whose path is shorter than 4 cm (thus overestimating the charge by a small amount since most of protons will cover a smaller path through the Particle material). A 100 g Particle of aluminium will have a radius of ≈ 2.07 cm.

It is advisable to determine first which charges (and fluxes that create them) might be neglected.

4.1. Admissible charges

Let us estimate the Coulomb interaction both between the Shepherd and the Particle and between each test body and its image in the capsule walls. To estimate the spurious effects on the Particle trajectory, it is reasonable to calculate its possible displacements due to the Coulomb forces from the growing number of captured charged particles. We assume that the test bodies are discharged by grounding to the capsule before launching the Particle in each given experiment.

Criterion. We will call the induced charges, or the fields they create, *admissible* if they cause a displacement of the Particle with respect to the Shepherd smaller than a prescribed coordinate measurement error δl (we take here $\delta l = 10^{-6}$ m) for a prescribed measurement time (we take $t \geq 10^4$ s).

The Coulomb acceleration $a_Q(t) = q_M q_m/(r^2 m)$ (in the Gaussian system of units) depends on the Shepherd-Particle separation r and on the form of the function $J(t)$, which in turn depends on the satellite orbital motion.

The charge-induced Particle displacement is approximately

$$\Delta l = \int dt \left[\int dt\, a_Q(t) \right] \tag{19}$$

since the acceleration is almost unidirectional. If, for estimation purposes, we suppose that the flux $J(t,x)$ is time-independent, then the resulting displacement is about

$$\Delta l \sim \frac{1}{30} \frac{e^2 S_M S_m J_0^2 t^4}{r^2 m}, \tag{20}$$

where $S_M \approx 1256$ cm^2 is the Shepherd cross-section, $S_m \approx 12.56$ cm^2 is the Particle cross-section, m is the Particle mass and r is an average Shepherd-Particle separation.

The strong time dependence is explained by the rapid growth of the Coulomb force due to growing charges. Numerically, with the above values of S_M and S_m, taking $m = 100$ g and $r = 1$ m (the latter leads to an overestimated force since the Particle spends most of time at greater distances), we find:

$$J_0^2 t^4 \lesssim 0.83{\cdot}10^{18} \text{ s}^2\text{cm}^{-4}. \tag{21}$$

For $t = 10^4$ s an admissible flux is thus less than 9 $\text{cm}^{-2}\text{s}^{-1}$.

Another undesired effect is that the Particle, being charged by the belt protons, will interact with the capsule walls. This is well approximated as an interaction with the Particle's mirror image in the wall, while the latter may be roughly imagined as a conducting plane. Then, assuming that the Particle is at average at about 25 cm from the capsule wall and using the same kind of reasoning as above, we obtain instead of (21)

$$J_0^2 t^4 \lesssim 2.07{\cdot}10^{19} \text{ s}^2\text{cm}^{-4} \tag{22}$$

and an admissible proton flux less than 45 $\text{cm}^{-2}\text{s}^{-1}$ for $t = 10^4$ s.

Some more estimates are of interest: if the charge can be kept smaller than a certain value, then what is the upper limit for it to create only negligible displacements? Suppose that there are constant charges on both the Shepherd ($q = q_M$) and the Particle ($q = q_m$, $m = 100$ g), then they are admissible according to the above criterion as long as

$$q_M q_m < 2{\cdot}10^{-6}\,\text{CGSE}_q{}^2 = \tfrac{2}{9}{\cdot}10^{-24}\ \text{C}^2, \tag{23}$$

$$q_m^2 < \tfrac{1}{2}{\cdot}10^{-6}\,\text{CGSE}_q{}^2. \tag{24}$$

These inequalities follow, respectively, from considering the Shepherd-Particle interaction and the interaction between the Particle (located at 25 cm from the wall) and its image. Thus the maximum admissible Particle charge is about $7{\cdot}10^{-4}$ $\text{CGSE}_q \approx 1.5{\cdot}10^6 e$; assuming this value, it follows from (23) that the maximum Shepherd charge is about $3{\cdot}10^{-3}$ $\text{CGSE}_q \approx 5.5{\cdot}10^6 e$. With these charge values the electric potentials on the test body surfaces are

$$U_M \approx 1.5{\cdot}10^{-4}\,\text{CGSE}_q/\text{cm} = 45 \text{ mV};$$
$$U_m \approx 3.5{\cdot}10^{-4}\,\text{CGSE}_q/\text{cm} = 105 \text{ mV}. \tag{25}$$

If by any means the requirements (23), (24) are satisfied (e.g., the potentials are kept smaller than the values (25)), the electrostatic effect on the Particle trajectory may be neglected.

The Shepherd's interaction with the respective image charge induced at nearest location to it in the SEE experimental chamber does not lead to appreciable Particle displacements. A very demanding requirements on the Shepherd's charge emerges, however, if the SEE satellite is used for G-dot determination (whose detailed discussion is postponed to future papers). For that case,

$$U_M \lesssim 1 \text{ mV}. \tag{26}$$

Table 2. Average flux, peak flux and captured charges per revolution in some satellite orbits

Orbit	Wall thickness	Average flux, $cm^{-2}s^{-1}$	Peak flux, $cm^{-2}s^{-1}$	Shepherd charge q_M	Particle charge q_m
1500b	2 cm	1420	12300	$1.5{\cdot}10^{10}$ e	$4.5{\cdot}10^{7}$ e
	4 cm	1000	8800	$1{\cdot}10^{10}$ e	$2.6{\cdot}10^{7}$ e
	6 cm	770	6800	$7.5{\cdot}10^{9}$ e	$1.5{\cdot}10^{7}$ e
	8 cm	600	5400	$6{\cdot}10^{9}$ e	$1.2{\cdot}10^{7}$ e
1500c	2 cm	646	5700	$6.5{\cdot}10^{9}$ e	$1.9{\cdot}10^{7}$ e
	4 cm	464	4200	$4.3{\cdot}10^{9}$ e	$1.1{\cdot}10^{7}$ e
	6 cm	365	3300	$3.5{\cdot}10^{9}$ e	$7{\cdot}10^{6}$ e
	8 cm	280	2700	$2.7{\cdot}10^{9}$ e	$5{\cdot}10^{6}$ e

Evidently, in this case the Shepherd-Particle interaction *per se* is not the determining factor with respect to charge limits on the test bodies.

4.2. The captured charges in certain orbits

The charges captured by the Shepherd and the Particle on board a satellite in various circular orbits for a single revolution around the Earth, a period of about two hours, were estimated in [25]. (Actual measurement times may exceed this period, but not by much.) These estimates were obtained with the aid of SEE2 and SEREIS software, created at Nuclear Physics Institute of Moscow State University [26].

The results obtained lead to some conclusions of importance for the SEE experiments (details see in [25]).

First, the models show zero proton fluxes in equatorial orbits of 500 — 800 km altitude but indicate considerable fluxes at the same altitudes due to crossing the SAA. It turns out, however, that the SAA is overwhelmingly a low-energy phenomenon and leaves the fluxes virtually unaffected on the relevant energy scale, beginning at approximately 65 MeV. Moreover, there is a very small proton flux due to the SAA even at energies above 10 MeV, hence, with 1 mm layer of shielding, the SAA influence is negligible. Behind a thicker layer of shielding there are actually no secondary particles due to SAA protons.

Second, at an altitude of 1500 km the fluxes depend substantially on the orbit orientation but remain on the same scale of a few million protons per cm^2 at energies over 65 MeV.

Third, at an altitude of 3000 km both the total flux (for $x = 0$) and its high-energy component in particular are evidently a few times greater than at 1500 km.

Fourth, and most important: for all orbits in the desirable range of altitudes the charges are quite large compared with their admissible values and they remain large even behind relatively thick walls. It is thus quite important to have means to detect and remove these charges during the measurements. Moreover, as seen from the peak values in Table 2 and time scans of Van Allen charging in orbits of interest (1500c is one of the most favourable ones, 1500b is less favourable; the data were also obtained using the above-mentioned software), at a charging peak when crossing the magnetic equator the time required for the charge on the test bodies to reach its maximum allowable values, as listed above, is a matter of seconds, not minutes. Therefore the charge must be detected and removed as it builds up, on a time scale of seconds.

The detection and measurement of the charge on the test bodies can probably be achieved relatively easily by an array of minute microvoltmeters attached to the inner wall of the experimental chamber.

Several methods for removing positive charge are now being evaluated. A simple and promising method may be to shoot electron beams directly at test bodies. The number of electrons needed is of the order of $10^8/s$. Although this approach has the inherent drawback that it requires that an active system must perform correctly for many years, it is simple in principle and will accomplish the goal.

5. Concluding remarks

The main results of the recent developments described in this paper may be summarized as follows:

1. Numerical simulations of the Particle relative motion in the case of a lighter Shepherd (200 kg), for initial Particle-Shepherd separations between 2 and 5 m, for $H_{\rm orb} = 500 \div 3000$ km, has shown that the sensitivity of trajectories with respect to changes of G did not change too much compared to the previous estimates with a heavier Shepherd (500 kg). In particular, variations $\delta G/G \sim 10^{-6}$ lead to trajectory shifts along the x axis ranging from $0.634{\cdot}10^{-6}$ to $3.34{\cdot}10^{-6}$ m.

It has been found that an error of 1 cm in $H_{\rm orb}$ leads to trajectory shifts of $3{\cdot}10^{-8}$ to 10^{-7} m, i.e., about an order of magnitude smaller than the planned coordinate measurement error, 10^{-6} m, and than the trajectory shifts due to G variations of 1 ppm.

An estimated error $\delta G/G$ due to Shepherd nonsphericity, characterized by its quadrupole moment

$J_2 \sim 10^{-5}$, is close to 10^{-6}; this implies rather severe requirements upon the Shepherd fabrication precision. The same quadrupole moment causes even greater $\delta G/G$ if the Particle motion starts at $y_0 > 15$ cm.

2. Computer simulations have shown that the gravitational constant G can be measured up to $\sim 5{\cdot}10^8$. The inverse square law may be tested with a sensitivity of $\alpha \sim 2{\cdot}10^{-7}$ for $\lambda = 1.2$ m and $\alpha \sim 3{\cdot}10^{-8}$ for $\lambda \sim 3.4{\cdot}10^6$ m (half the Earth's radius). Observation of the Shepherd orbit precession makes it possible to test the inverse square law at $\lambda \sim 3.4{\cdot}10^5$ m up to 10^{-10}.

3. Estimation of test body charging due to crossing the van Allen radiation belts shows that this effect requires special means for charge measuring and removal. These means, however, do not go beyond the presently available technology level.

Acknowledgement

This work was supported in part by NASA grant # NAG 8-1442. K.A.B. wishes to thank Nikolai V. Kuznetsov for helpful discussions and for providing access to the SEE2 and SEREIS software. V.N.M. is grateful to CINVESTAV and CONACYT for their hospitality and support during his stay in Mexico.

References

[1] A.J. Sanders and W.E. Deeds, Phys. Rev. **D 46** , 480 (1992).

[2] V. de Sabbata, V.N. Melnikov and P.I. Pronin, "Theoretical Approach to Treatment of Nonnewtonian Interactions", *Progr. Theor. Phys.* **88**, 623 (1992).

[3] V.N. Melnikov, *Int. J. Theor. Phys.* **33**, 7, 1569 (1994).

[4] G.T. Gillies, *Rep. Progr. Phys.* **60** , 151 (1997).

[5] M.P. Fitzgerald and T.R. Armstrong, "Recent Results for g from MSL Torsion Balance", *in:* "The Gravitational Constant: Theory and Experiment 200 Years after Cavendish" (23-24 Nov. 1998), Abstracts (Cavendish–200 Abstracts), Inst. of Physics, London, 1998.

[6] J. Schurr, F. Nolting and W. Kündig, *Phys. Rev. Lett.* **80**, 1142 (1998).

[7] H. Meyer, "Value for G Using Simple Pendulum Suspensions", *in:* Cavendish–200 Abstracts. "The Gravitational Constant: Theory and Experiment 200 Years after Cavendish" (23-24 Nov. 1998), Abstracts, Inst. of Physics, London, 1998.

[8] O.V. Karagioz, V.P. Izmaylov and G.T. Gillies, *Grav. & Cosmol.* **4**, 3, 239 (1998).

[9] J.H. Gundlach and S.M. Merkowitz, *Phys. Rev. Lett.* **85**, 2869 (2000).

[10] E. Fischbach and C. Talmage, *Mod. Phys. Lett.* **A4**, 2303 (1989); *Nature (London)* **356**, 207 (1992).

[11] E. Fischbach and C. Talmage, "Twelve Years of the Fifth Force". In: "Int. Workshop on Gravitation and Astrophysics", Tokyo, Japan, 17-19 Nov. 1997, p. 1–9.

[12] P.G. Roll, R. Krotkov and R.H. Dicke, *Ann. Phys. (N.Y.)* **26**, 442 (1964).

[13] V.B. Braginsky and V.I. Panov, *ZhETF* **61**, 873 (1971) [*Sov. Phys. JETP* **34**, 463 (1972)].

[14] V. Achilli et al., "A geophysical experiment on Newton's inverse-square law," *Nuovo Cim.* **112B**, 5, 775 (1997).

[15] E.G. Adelberger, "Modern tests of the universality of free fall"; *Class. Quantum Grav.* **11** , A9–A21 (1994).

[16] E. Fischbach, G.T. Gillies, D.E. Kraus, J.G. Schwan, and C. Talmadge, "Non-Newtonian gravity and new weak forces: an index of measurement and theory"; *Metrologia* **29** , 3, 13–260 (1992).

[17] A. Franklin, "The Rise and Fall of the Fifth Force: Discovery, Pursuit, and Justification in Modern Physics", American Institute of Physics, N.Y., 1993.

[18] A.D. Alexeev, K.A. Bronnikov, N.I. Kolosnitsyn, M.Yu. Konstantinov, V.N. Melnikov and A.G. Radynov, *Izmeritel'naya Tekhnika,* 1993, No. 8, 6; No. 9, 3; No. 10, 6; 1994, No. 1, 3;

[19] A.D. Alexeev, K.A. Bronnikov, N.I. Kolosnitsyn, M.Yu. Konstantinov, V.N. Melnikov and A.G. Radynov, *Int. J. Mod. Phys.* **D 3**, 4, 773 (1994).

[20] N.A. Zaitsev and N.I. Kolosnitsyn. *In:* "Experimental Tests of Gravitation Theory", Moscow University Press, 1989, p.38–50 (in Russian).

[21] B.A. Tverskoy, "Dynamics of the Earth's Radiation Belts", Moscow, Nauka, 1968 (in Russian).

[22] Yu.I. Galperin, L.S. Gorn and B.I. Khazanov, "Radiation Measurements in Space", Moscow, Atomizdat, 1972 (in Russian).

[23] D.J. Williams, ESSA Technical Report ERL 180-SDL16, 1970.
A.J. Dessler and B.J. O'Brien, "Penetrating Particle Radiation", *in:* "Satellite Environment Handbook", 2nd edition, ed. F.S. Johnson, Stanford University Press, Stanford, CA, 1965, p. 53–92.

[24] W.N. Hess, "The Radiation Belt and Magnetosphere", Ginn Blaisdell, Waltham, MA, 1968.

[25] A.D. Alexeev, K.A. Bronnikov, N.I. Kolosnitsyn, M.Yu. Konstantinov, V.N. Melnikov and A.J. Sanders. "SEE Project: Current Status and New Estimates", *Grav. & Cosmol.* **5**, 1, 67-78 (1999).

[26] V.F. Bashkirov, N.V. Kuznetsov and R.A. Nymmik, "Information system for evaluation of space radiation environment and radiation effects on spacecraft". Workshop "Space Radiation Environment Modelling: New Phenomena and Approaches", Oct. 7–9, 1997: Program and Abstracts, p. 4.8.

[27] S. Brandt, "Statistical and Computational Methods in Data Analysis", Heidelberg Univ. Press, 1970.